inventions

MDPI

Article

Applications of the Order Reduction Optimization of the H-Infinity Controller in Smart Structures

Amalia Moutsopoulou [1], Markos Petousis [1,*], Nectarios Vidakis [1], Georgios E. Stavroulakis [2] and Anastasios Pouliezos [2]

[1] Department of Mechanical Engineering, Hellenic Mediterranean University, 71410 Heraklion, Greece; amalia@hmu.gr (A.M.); vidakis@hmu.gr (N.V.)
[2] Department of Production Engineering and Management, Technical University of Crete, 73100 Chania, Greece; gestavr@dpem.tuc.gr (G.E.S.); tasos@dpem.tuc.gr (A.P.)
* Correspondence: markospetousis@hmu.gr; Tel.: +30-2810379227

Abstract: In this paper, our strategy is to look for locally optimum answers to a non-smooth optimization problem that has been constructed to include minimization goals and restrictions for smart structures' vibration suppression. In both theoretical analysis and practical implementation, it is widely recognized that designing multi-objective control systems poses a considerable challenge. In this study, we assess the effectiveness of this method by employing the open-source Matlab toolbox Hifoo 2.0 and juxtapose our findings with established industry standards. We start by framing the control problem as a mathematical optimization issue and proceed to identify the controller that effectively addresses this optimization. This approach introduces the potential application of intelligent structures in tackling the challenge of vibration suppression. This study makes use of the most recent version of the freely available application Hifoo which tries to study vibration suppression with the limits outlined above in the context of multi-objective controller design. A controller directive is initially set, allowing for a lower order.

Keywords: optimization problem; H-infinity controller; Hifoo control; smart structures

Citation: Moutsopoulou, A.; Petousis, M.; Vidakis, N.; Stavroulakis, G.E.; Pouliezos, A. Applications of the Order Reduction Optimization of the H-Infinity Controller in Smart Structures. *Inventions* **2023**, *8*, 150. https://doi.org/10.3390/inventions8060150

Academic Editors: Peng Du, Haibao Hu and Xiaopeng Chen

Received: 18 October 2023
Revised: 18 November 2023
Accepted: 21 November 2023
Published: 22 November 2023

1. Introduction

In recent years, there has been a lot of interest in piezoelectrically activated smart structures that have robust vibration control. For systems that must maintain stability or performance in the face of several sources of uncertainty, such control rules are ideal [1–4]. The later robust controller leads to an appropriate design of smart structures by accounting for the uncertainties of the dynamical system and the incompleteness of the measured data. The numerical simulation demonstrates that the general methods proposed can effectively suppress vibration in the case of a piezoelectric smart structure, serving as a tutorial. The ultimate goal of this approach is to provide a comprehensive and unique methodology for the design and validation of robust H-infinity controllers for active structures [5–9].

The implementation of active control technologies in intelligent structures has been the focus of the current effort. In addition to vibration reduction, low steady-state error, fast recovery, and little-to-no maximum uplift are also desired; nevertheless, control energy cannot go beyond operational bounds. H-infinity control has the benefit of allowing the computation to account for the worst-case scenario of unpredictable disturbances and system noise. Furthermore, a wide frequency spectrum may be created as the H-infinity controller can effectively handle more input. The findings are noteworthy; vibration reduction is demonstrated even for actual wind loads when the voltage of the piezoelectric component is regulated within tolerance. Utilizing the Hifoo controller in conjunction with non-parametric and non-convex optimization methods. The results are good; we completely reject disturbances utilizing reduced-order control and H-infinity control [10–15]. The aforementioned discusses the many control techniques used to reduce noise and vibration

in structures. This study contributes to the use of control to reduce intelligent structures' oscillations. The main advancement is the use of a reduced-order controller to achieve total oscillation suppression.

In this research, we first make use of the H-infinity control implementations in smart structures. A controller based on H-infinity is intended to inhibit the smart piezoelectric structure's vibration under dynamic loading. It is demonstrated that the H-infinity controller is resilient to parametric uncertainty in vibration suppression situations. The advantages of active vibration suppression and robust control in smart structure dynamics are clearly described in this paper. Robust control theory is needed to develop smart structure controllers that deliver stability with guaranteed performance [1–3]. A disadvantage of controller H infinity is the large computational demands, especially when the number of finite elements increases. By using the controller, we can get just as good results as a reduced-order controller. Second, the most current version of the publicly accessible program, Hifoo [4–7], which aims to overcome the limitations mentioned above in the context of multi-objective controller design, is used in this study. Compared to traditional control approaches, Hifoo methods offer the benefit of being immediately adaptable to difficulties with multivariate systems. It is challenging to optimize both great performance and stability at the same time [7–13]. The behavior of a pair of piezoelectric patches applied symmetrically to the top and bottom surfaces of each beam element will be studied in an intelligent cantilever smart construction. No lifting or Lyapunov variables are used to address the requirements' incompatibilities. This leads to an optimization issue that is often short-dimensional, non-smooth, and nonconvex, and does not need the solution of any significant convex subproblems [4–7]. It is usually simple to locate an appropriate controller rather than an efficient robust control in reality, even though the behavior of this technique cannot be guaranteed [8–10]. Hifoo methods have the advantage of being quickly adaptive to problems involving multivariate systems in comparison to typical control approaches. Optimizing strong stability and performance at the same time is difficult [11–13]. A method known as Hifoo loop-shaping allows the control designer to use typical loop-shaping techniques to the multivariable frequency response in order to achieve beneficial robust performance, before optimizing the response near the system bandwidth to meet good robust criteria. In this article [12,14,15], the benefits of strong control in intelligent companies are discussed.

Very high-order controllers are often produced by most of the techniques or heuristics currently used to address these issues. The control behavior of the beam matches predictions, and the results show the effectiveness of the provided model and method. The beam's control behavior is in line with expectations, and the outcomes demonstrate the effectiveness of the suggested model and procedure. In this work, a beam with piezoelectric patches is controlled and oscillations caused under dynamic load are reduced. In recent years, there has been a lot of interest in piezoelectrically activated smart structures that have robust vibration control. The Hifoo robust controller leads to an appropriate design of smart structures by accounting for the uncertainties of the dynamical system and the incompleteness of the measured data. The numerical simulation demonstrates that the general methods proposed can effectively suppress vibration in the case of a piezoelectric smart structure, serving as a tutorial. The ultimate goal of this approach is to provide a comprehensive and unique methodology for the design and validation of robust Hifoo controllers for active structures [16–20]. The findings are remarkable; even for actual wind loads, vibration reduction is shown when the piezoelectric component voltage is adjusted tolerably. In order to reduce the model's processing requirements, the controller rank was dropped by combining non-parametric and nonconvex optimization approaches with the Hifoo controller. Both the local bundle technique and the gradient sampling method cannot be employed if the MATLAB route lacks the quadratic programming tool "quadprog". These three optimization techniques each make use of the gradients that Hifoo dynamically produces. Finding the odd locations where gradients do not exist is not attempted. The positions of the gradient discontinuities do not cause the procedures to fail. The latter

phases of the bundle and gradient sampling look for a place where a convex combination of gradients at neighboring points has a small norm. Even with a substantially lower system degree, the controller functioned flawlessly. Strong stabilization, in which a robust controller must stabilize a plant, and simultaneous stabilization, in which a single controller must be discovered to stabilize many plants, are characteristic instances of multi-objective robust control issues [7,16,17]. We evaluate the system's flexibility and durability after doing a system analysis. The beneficial aspects of this work are as follows: reduced-order optimization of the H-infinity controller in intelligent structures, control of oscillation suppression by simulating intelligent entities, results in the time–space domain and the frequency domain, application of measurement noise of beam state, complete suppression of oscillations, reduction of controller order, input of white noise as disturbance input, taking it as a percentage of the disturbances, and application of measurement noise. The results are excellent. We achieved complete disturbance rejections with H-infinity control and with reduced-order control. The following are alternative control techniques used to reduce structural noise and vibration. This work contributes to the application of control to reduce the oscillations of smart structures. The innovation is that full suppression of oscillations is achieved with a reduced-order controller. In other words, the optimal result is achieved with much smaller computational requirements and without compromising the accuracy of the model. The first focus of future studies will be on how to apply these certain command techniques to real intelligent structures in an experimental context. This article presents innovations in the application of the demanding theory of control to smart materials and computational mechanics. The innovation is that full suppression of oscillations is achieved with a reduced-order controller. In other words, the optimal result is achieved with much smaller computational requirements and without compromising the accuracy of the model.

2. Methodology

2.1. Controller Synthesis H-Infinity

The aforementioned provides ways for comparing and assessing controller performance as well as answers to analytical difficulties. Nonetheless, it is feasible to approximately synthesize a controller that delivers a specific performance in terms of the structured single -μ- value. In this procedure known as (D, G-K) iteration [17–22], i.e., the difficulty in identifying a μ-optimal controller K so that $\mu(F(j\omega), K(j\omega)) \leq \beta, \forall\omega$, is converted into the problem of identifying finding transfer function matrices $D(\omega)\in$ and $G(\omega)\in{}_{\infty}$, such that,

$$\sup_{\omega}\overline{\sigma}\left[\left(\frac{D(\omega)\left(F_u(F(j\omega),K(j\omega))D^{-1}(\omega)\right.}{\gamma}-jG(\omega)\right)\left(I+G^2(\omega)\right)^{-\frac{1}{2}}\right]\leq 1,\forall\omega \quad (1)$$

Unfortunately, this approach fails to provide any guarantee of identifying local maxima. However, a method referred to as D-K iteration is available for complicated perturbations (additionally implemented in MATLAB). It connects H-infinity synthesis and μ-analysis generally, producing positive outcomes. The initial reference is a limit on μ expressed in relation to the adjusted singular value [22,23],

$$\mu(N)\leq\min_{D\in D}\overline{\sigma}\left(DND^{-1}\right) \quad (2)$$

The concept aims to identify a controller that minimizes the maximum value over the frequency of its upper bound, namely,

$$\min_{K}\left(\min_{D\in D}\left\|DN(K)D^{-1}\right\|_{\infty}\right) \quad (3)$$

by taking turns in the process of minimizing $\left\|DN(K)D^{-1}\right\|_{\infty}$ with respect to either K or D (while maintaining the other fixed) [21,23–26].

The challenge is the process of selecting a single controller using state-space equations, $K = (A_K, B_K, C_K, D_K)$. The maximum 2-norm perturbation to a stable closed loop system that may be accepted whilst still ensuring that the perturbed system stays stable is the H-infinity norm, which is not specified. The biggest real component of a closed loop system's poles (eigenvalues) is called the spectral abscissa.

To exhibit P in state space, the natural partitioning must be generated,

$$P(s) = \begin{bmatrix} A & B_1 & B_2 \\ C_1 & D_{11} & D_{12} \\ C_2 & D_{21} & D_{22} \end{bmatrix} = \begin{bmatrix} P_{zw}(s) & P_{zu}(s) \\ P_{yw}(s) & P_{yu}(s) \end{bmatrix} \tag{4}$$

where the packed form has been used, while the equivalent type for K is,

$$K(s) = \begin{bmatrix} A_K & B_K \\ C_K & D_K \end{bmatrix} \tag{5}$$

Equation (4) specifies the equations,

$$\begin{gathered} \dot{x}(t) = Ax(t) + \begin{bmatrix} B_1 & B_2 \end{bmatrix} \begin{bmatrix} w(t) \\ u(t) \end{bmatrix} \\ \begin{bmatrix} z(t) \\ y(t) \end{bmatrix} = \begin{bmatrix} C_1 \\ C_2 \end{bmatrix} x(t) + \begin{bmatrix} D_{11} & D_{12} \\ D_{21} & D_{22} \end{bmatrix} \begin{bmatrix} w(t) \\ u(t) \end{bmatrix} \end{gathered} \tag{6}$$

and,

$$\begin{gathered} \ddot{x}_\kappa(t) = A_\kappa x_\kappa(t) + B_\kappa y(t) \\ u(t) = C_\kappa x_\kappa(t) + D_\kappa y(t) \end{gathered} \tag{7}$$

To find the matrices involved, we break the feedback loop and use the relevant equations, in order to receive the structure in state space form, and align the inputs, outputs, states, and input/output to the controller:

$$\begin{gathered} \dot{x}_F = Ax_F + (Gd + Bu),\ x = Ix_F \\ \dot{x}_u = A_u x_u + B_u u,\ u_w = C_u x_u + D_u u \\ \dot{x}_e = A_e x_e + B_e J x,\ e_w = C_e x_e + D_e J x \\ \dot{x}_{nw} = A_{nw} x_{nw} + B_{nw} n_w,\ n = C_{nw} x_{nw} + D_{nw} n_w \\ \dot{x}_{dw} = A_{dw} x_{dw} + B_{dw} d_w,\ d = C_{dw} x_{dw} + D_{dw} d_w \\ y = Cx + n \end{gathered} \tag{8}$$

Let,

$$x = \begin{bmatrix} x_F \\ x_u \\ x_e \\ x_{nw} \\ x_{dw} \end{bmatrix},\ y = y,\ w = \begin{bmatrix} d_w \\ n_w \end{bmatrix},\ z = \begin{bmatrix} u_w \\ e_w \end{bmatrix},\ u = u \tag{9}$$

The internal signals d, n, and e x are substituted into Equation (8) to produce,

$$\begin{bmatrix} \dot{x}_F \\ \dot{x}_u \\ \dot{x}_e \\ \dot{x}_{nw} \\ \dot{x}_{dw} \end{bmatrix} = \begin{bmatrix} A & 0 & 0 & 0 & GC_{dw} \\ 0 & A_u & 0 & 0 & 0 \\ B_e J & 0 & A_e & 0 & 0 \\ 0 & 0 & 0 & A_{nw} & 0 \\ 0 & 0 & 0 & 0 & A_{dw} \end{bmatrix} \begin{bmatrix} x_F \\ x_u \\ x_e \\ x_{nw} \\ x_{dw} \end{bmatrix} + \begin{bmatrix} GD_{dw} & 0 \\ 0 & 0 \\ 0 & 0 \\ 0 & B_{nw} \\ B_{dw} & 0 \end{bmatrix} \begin{bmatrix} d_w \\ n_w \end{bmatrix} + \begin{bmatrix} B \\ B_u \\ 0 \\ 0 \\ 0 \end{bmatrix} u \tag{10}$$

$$\begin{bmatrix} u_w \\ e_w \end{bmatrix} = \begin{bmatrix} 0 & C_u & 0 & 0 & 0 \\ D_e J & 0 & C_e & 0 & 0 \end{bmatrix} \begin{bmatrix} x_F \\ x_u \\ x_e \\ x_{nw} \\ x_{dw} \end{bmatrix} + 0 \begin{bmatrix} d_w \\ n_w \end{bmatrix} + \begin{bmatrix} D_u \\ 0 \end{bmatrix} u \tag{11}$$

$$y = \begin{bmatrix} C & 0 & 0 & C_{nw} & 0 \end{bmatrix} \begin{bmatrix} x_F \\ x_u \\ x_e \\ x_{nw} \\ x_{dw} \end{bmatrix} + \begin{bmatrix} 0 & D_{nw} \end{bmatrix} \begin{bmatrix} d_w \\ n_w \end{bmatrix} + 0u \tag{12}$$

Therefore, the matrices are:

$$\begin{gathered} = \begin{bmatrix} A & 0 & 0 & 0 & GC_{dw} \\ 0 & A_u & 0 & 0 & 0 \\ B_eJ & 0 & A_e & 0 & 0 \\ 0 & 0 & 0 & A_{nw} & 0 \\ 0 & 0 & 0 & 0 & A_{dw} \end{bmatrix}, B_1 = \begin{bmatrix} GD_{dw} & 0 \\ 0 & 0 \\ 0 & 0 \\ 0 & B_{nw} \\ B_{dw} & 0 \end{bmatrix}, B_2 = \begin{bmatrix} B \\ B_u \\ 0 \\ 0 \\ 0 \end{bmatrix} \\ C_1 = \begin{bmatrix} 0 & C_u & 0 & 0 & 0 \\ D_eJ & 0 & C_e & 0 & 0 \end{bmatrix}, D_{11} = 0, D_{12} = \begin{bmatrix} D_u \\ 0 \end{bmatrix} \\ C_2 = \begin{bmatrix} C & 0 & 0 & C_{nw} & 0 \end{bmatrix}, D_{21} = \begin{bmatrix} 0 & D_{nw} \end{bmatrix}, D_{22} = 0 \end{gathered} \tag{13}$$

As can be seen, the state vector in this design has a size of 16 + 4 + 4 + 4 + 8 = 36. Modeling the controller K(s)'s size is additionally determined by this. In cases where any weight matrices are constant, this number will be reduced by the appropriate order [20,27,28].

The challenge is to select a single controller K = (A_K, B_K, C_K, D_K) that has state-space equations $A_K \in R^{nK \times nK}$, with B_K, C_K, and D_K that have compatible dimensions with AK and the generalized plant matrices. The designer can specify the controller order K since it is fixed [29–32]. For a stable closed-loop system, the complex stability radius is the largest 2-norm perturbation that is tolerable whilst still ensuring that the disrupted mechanism continues to be stable when the w and z performance channels are not specified, and the H-infinity norm is not defined [32–35]. A closed loop system's spectral abscissa is the biggest real component of its poles (eigenvalues).

2.2. Optimization Method Hifoo

A two-phase algorithm is used. The quasi-Newton approach (BFGS optimization algorithm), which is effective for nonconvex, non-smooth optimization, is the main driving force behind each phase [4–7]. If the user does not provide a first estimate for the desired controller, Hifoo produces the first controllers at random. Even if the user does make an initial guess, Hifoo nonetheless generates more initial controllers at random just in case they give better results. Lowering the closed loop plants' maximum spectral abscissa using BFGS is the first step in stabilizing. Once one is discovered that stabilizes these plants, the procedure concludes and a starting point for the second phase with a finite controller is attained. Increasing the penalty factor, while optimization is repeated as necessary if BFGS is unable to find a site where the constraint violations are zero (unless F is identically zero, in which case all j are finite). Although this method is frequently quick and extremely successful, there are no guarantees. By default, Hifoo follows BFGS using the more time-consuming Burke et al.'s [7] gradient sampling strategy; however, this may be altered.

2.3. Problem Formulation and Optimization Method

More information is provided in the equations of a generalized plant G's state-space.

$$\begin{gathered} \dot{x}(t) = Ax(t) + B_1w(t) + B_2u(t), \\ z(t) = C_1x(t) + D_{11}w(t) + D_{12}u(t), \\ y(t) = C_2x(t) + D_{21}w(t) + D_{22}u(t) \end{gathered} \tag{14}$$

and the controller K(s)'s state-space realization is

$$\begin{gathered} \dot{x}_K(t) = A_K\, x_K(t) + B_Ky(t), \\ u(t) = C_K\, x_K(t) + D_Ky(t), \end{gathered} \tag{15}$$

where $A \in R^{n \times n}$, $D_{12} \in R^{p1 \times m2}$, $D_{21} \in R^{p2 \times m1}$, with additional matrices that share equal dimensions, and $A_K \in R^{nK \times nK}$, with B_K, C_K, D_K A_K and the generalized plant matrices comparable in terms of dimensions. Because the order of the control is fixed, the designer is able to specify it.

The signals (z, w, y, u) stand in for the controlled outputs, exogenous inputs (such as disturbances and directives), measured inputs (or sensor inputs), and control inputs, in that order. T_{zw} stands for the transfer function from the input w to the output z; for further information, see [14]. The closed loop H∞ typical function can be minimized to represent the ideal H-infinity controller architecture.

$$\underset{K \text{ stabilizing}}{\text{Inf}} \quad \|T_{zw}\|_\infty,$$

in which K(s) internally stabilize the closed-loop system according to the restriction.

We apply the extra requirement that the controller be stable in this study because we want to decrease

$$\underset{K \text{ stabilizing and } K \text{ stable}}{\text{Inf}} \quad \|T_{zw}\|_\infty,$$

Let us use a(X) to represent the biggest real part of the eigenvalues, or the spectral abscissa of matrix X. As a result, we need both that $\alpha(A_{CL}) < 0$ and that $\alpha(A_K) < 0$ where A_{CL} is the closed-loop system matrix. The set of stable matrices, which is the feasible set for A_K, is not convex and has a rough boundary. It has received substantial research; for examples, see [5–7].

The two processes used by Hifoo are stability and performance optimization, just like in earlier versions [7,33]. As the closed-loop system is being stabilized, Hifoo 2 keeps minimizing $\max(\alpha(A_{CL}, \varrho\alpha(A_K))$, which is a positive parameter that will result in detaining more details subsequently, until it discovers a controller K for which this number is negative, indicating that the controller is stable. If Hifoo is unable to discover a suitable controller, it will return with an output to that effect.

Hifoo 2 searches for a local minimizer during the performance optimization phase of

$$f(K) = \begin{cases} \infty \text{ if } \max(\alpha(ACL),\ \alpha(AK)) \geq 0 \\ \max(\|T_{zw}\|_\infty \infty, \in \|K\|_\infty) \text{ otherwise} \end{cases} \tag{16}$$

where,

$$\|K\|_\infty = \sup_{\mathcal{R}\int=0} \left\| C_K(sI - A_K)^{-1}B_K + D_K \right\|_2.$$

The primary design objective aims to minimize the transfer function Tzw and stabilize the closed-loop system, so the introduction is justified. However, the K term restrains the H-infinity norm of the controller from growing too large, a condition that the stability constraint alone cannot ensure. The performance phase of optimization starts with f (K), obtaining a bounded value because of the stabilization phase. The rejection occurs during the line search process, which demands a decrease in the objective function at each iteration. The optimization algorithm that Hifoo [36] calls at each level employs the non-smooth, nonconvex optimization technique known as HANSO. These components make up its composition: if a local bundle approach fails to identify local optimality for the best point determined by BFGS, gradient sampling [2,4] tries to enhance the local minimizer's estimate and returns a rough optimality value. To approximate a local minimizer faster, we use a quasi-Newton algorithm (BFGS). If the MATLAB route does not contain the quadratic programming tool "quadprog", neither the local bundle approach nor the gradient sampling method is used [34,36–38]. Each of these three methods of optimization takes advantage of the gradients that Hifoo dynamically generates. Identifying the peculiar places where the gradients do not exist is not attempted. The methods do not fail as a result of the gradient discontinuities at unusual locations. The last stages of the bundle and gradient sampling search parameter space for a location where a convex combination of gradients at nearby points has a small norm. The algorithm is two-phase. Each phase is mainly driven by the

quasi-Newton technique (BFGS optimization algorithm), which is efficient for nonconvex, non-smooth optimization [4–7]. Hifoo generates the initial controllers at random if the user does not supply a first estimate for the desired controller. Hifoo produces more initial controllers at random even if the user does make an initial estimate, just in case they produce better results. The first step in stabilizing is lowering the maximum spectral abscissa of the closed loop plants using BFGS. The process is complete and a starting point for the second phase with a finite controller is reached once one is found that stabilizes these plants. Increasing the penalty factor and repeating optimization, as necessary. A very poorly conditioned Hessian approximation matrix is produced during the BFGS phase. There is further information in [4–7,39].

3. Results

3.1. Application in Smart Structures

The following part will analyze the behavior of an eight-element cantilever smart structure with symmetrical bonds between four pairs of piezoelectric patches at each beam element's top and bottom surfaces (Figures 1 and 2). The different components of this construction have the dimensions presented below.

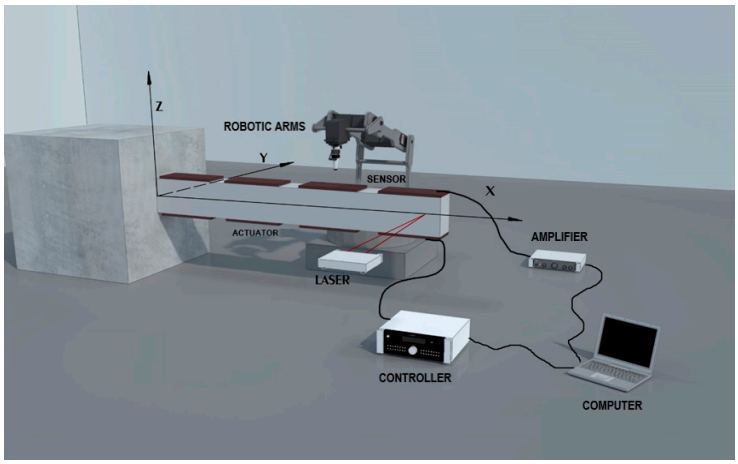

Figure 1. Intelligent structure.

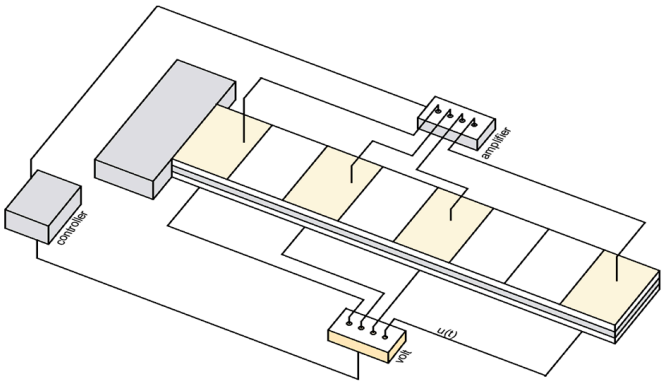

Figure 2. Piezoelectric smart beam.

The dynamical description of the system is provided by

$$M\ddot{q}(t) + C\dot{q} + Dq(t) = f_m(t) + f_e(t) \quad (17)$$

where M is the global mass matrix, C is the viscous damping matrix, D represents the global stiffness matrix, f_m represents the global external loading vector, and f_e is the global control

force vector produced by electromechanical coupling effects. The independent variable q(t) is composed of transversal deflections w_i and rotations ψ_i, i.e.,

$$q(t) = \begin{bmatrix} w_1 \\ \psi_1 \\ \vdots \\ w_n \\ \psi_n \end{bmatrix} additionally \tag{18}$$

in which n is the number of finite elements that the analysis is using. Vectors w and $\mathbf{f}_m$ is positive upwards.

In order to convert to state-space control representation, allow (in the usual manner)

$$x(t) = \begin{bmatrix} q(t) \\ \dot{q}(t) \end{bmatrix} \tag{19}$$

Additionally, to define $f_e(t)$ as Bu(t), we express it as $F_e^* u$, where F_e^* (of size $2n \times n$) is the piezoelectric force for a unit applied on the corresponding actuator, and u stands for the voltages on the actuators [40–42]. Lastly, $d(t) = f_m(t)$ is the disturbance vector. Then,

$$\begin{aligned} \dot{x}(t) = \begin{bmatrix} 0_{2n\times 2n} & I_{2n\times 2n} \\ -M^{-1}K & -M^{-1}D \end{bmatrix} x(t) + \begin{bmatrix} 0_{2n\times n} \\ M^{-1}F_e^* \end{bmatrix} u(t) + \begin{bmatrix} 0_{2n\times 2n} \\ M^{-1} \end{bmatrix} d(t) \\ = Ax(t) + Bu(t) + Gd(t) \\ = Ax(t) + \begin{bmatrix} B & G \end{bmatrix} \begin{bmatrix} u(t) \\ d(t) \end{bmatrix} \\ = Ax(t) + B\widetilde{u}(t) \end{aligned} \tag{20}$$

This can be enhanced using the output equation (displacements only measured),

$$y(t) = [x_1(t)\ x_3(t) \ldots x_{n-1}(t)]^T = Lx(t) \tag{21}$$

In this formulation u is $n \times 1$ (at most, but can be smaller), while d is $2n \times 1$, (n is the number of nodes). The units used are m, rad, sec, and N. The parameters of the smart beam are in Table 1. Our system remains stable in the field of time-space, but stability is presented in more detail in the field of frequency domain.

Table 1. Parameters of the smart beam.

Parameters	Values
L, for beam length	1.00 m
W, for Beam Width	0.002 m
Wp, PZT Width	0.002 m
h, for Beam thickness	0.096 m
hp, piezoelectric thickness	0.0002 m
ρ, for Beam density	1600 kg/m^3
E, for Young's modulus of the beam Ep, Young modulus of pzt 6.3×10^{10} N/m^2	1.5×10^{11} N/m^2
bs, ba, for PZT thickness	0.002 m
d_{31} the Piezoelectric constant	230×10^{-12} m/V

3.2. Results for H-Infinity Control

The Matlab routine for H-infinity control is: [Kinf] = h_{inf}syn(sysic, nmeas, ncont),

Where nmeas = 4 is the number of sensors, ncont = 4 is the number of the controller, and sysic is the formulation of the block diagram. In Figure 3 for this formulation, we use the Matlab code:

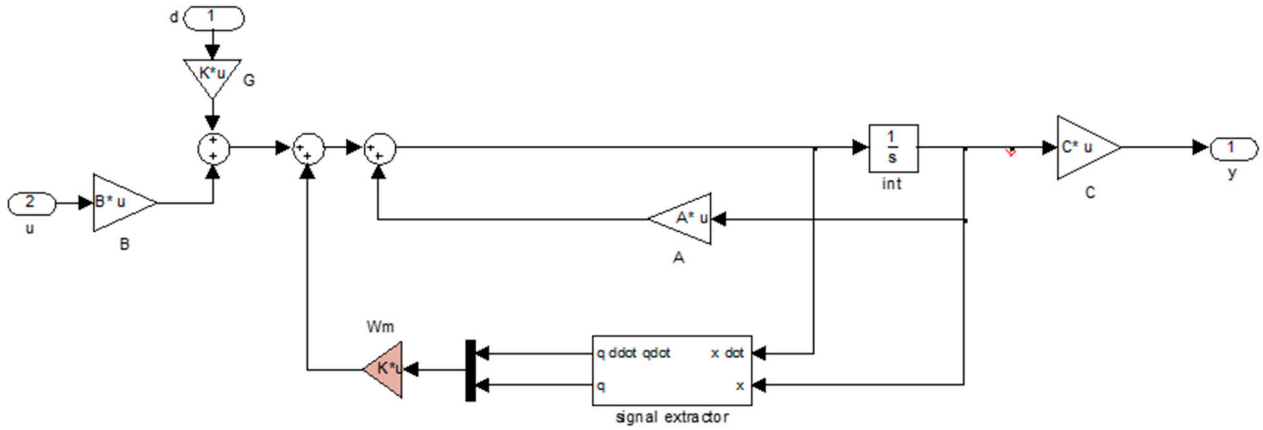

Figure 3. Block diagram in Simulink for the smart beam (* is × in the diagram).

```
beam0 = ss(A0, eye(2+nd), eye(2+nd), 0);
y = C0;
systemnames = ' beam0 y ad su se We Wu Wn ';
inputvar = '[ n(4); d(8); u(4)]';
input_to_sd = '[Wd]';
input_to_su = '[u]';
input_to_se = '[beam0]';
input_to_beam0 = '[ sd+su ]';
input_to_y = '[ beam0 ]';
input_to_Wu = '[u]';
input_to_Wn = '[n]';
input_to_Wd = '[d]';
input_to_We = '[se]';
```

The whetted matrix for noise, control, error, and disturbance are for control u:

$$W_{u=}\begin{bmatrix} \frac{5.556\times10^{-6}s+0.005556}{s+100} & 0 & 0 & 0 \\ 0 & \frac{5.556\times10^{-6}s+0.005556}{s+100} & 0 & 0 \\ 0 & 0 & \frac{5.556\times10^{-6}s+0.005556}{s+100} & 0 \\ 0 & 0 & 0 & \frac{5.556\times10^{-6}s+0.005556}{s+100} \end{bmatrix} \quad (22)$$

For error e:

$$W_{e=}\begin{bmatrix} \frac{2513}{s+31.42} & 0 & 0 & 0 \\ 0 & \frac{2513}{s+31.42} & 0 & 0 \\ 0 & 0 & \frac{2513}{s+31.42} & 0 \\ 0 & 0 & 0 & \frac{2513}{s+31.42} \end{bmatrix} \quad (23)$$

For disturbances d:

$$W_{d=}\begin{bmatrix} 40 & 0 & 0 & 0 & 0 & 0 & 0 & 0 \\ 0 & 40 & 0 & 0 & 0 & 0 & 0 & 0 \\ 0 & 0 & 40 & 0 & 0 & 0 & 0 & 0 \\ 0 & 0 & 0 & 40 & 0 & 0 & 0 & 0 \\ 0 & 0 & 0 & 0 & 40 & 0 & 0 & 0 \\ 0 & 0 & 0 & 0 & 0 & 40 & 0 & 0 \\ 0 & 0 & 0 & 0 & 0 & 0 & 40 & 0 \\ 0 & 0 & 0 & 0 & 0 & 0 & 0 & 40 \end{bmatrix} \quad (24)$$

For noise n:

$$W_{n=}\begin{bmatrix} 10^{-6} & 0 & 0 & 0 \\ 0 & 10^{-6} & 0 & 0 \\ 0 & 0 & 10^{-6} & 0 \\ 0 & 0 & 0 & 10^{-6} \end{bmatrix} \quad (25)$$

In all simulations the input is also white noise as the disturbance input, taking it as a percentage of the measurement (in Matlab Simulink) Figure 4. In all the simulations that have been done in Matlab, noise has been obtained in the measurements +, − one percent as a percentage of the signal input. This was done to take into account uncertain disturbances of the system, for example, unpredictable disturbances of the air force. The system was tested in the Simulink Matlab, and the model used is shown in Figure 4.

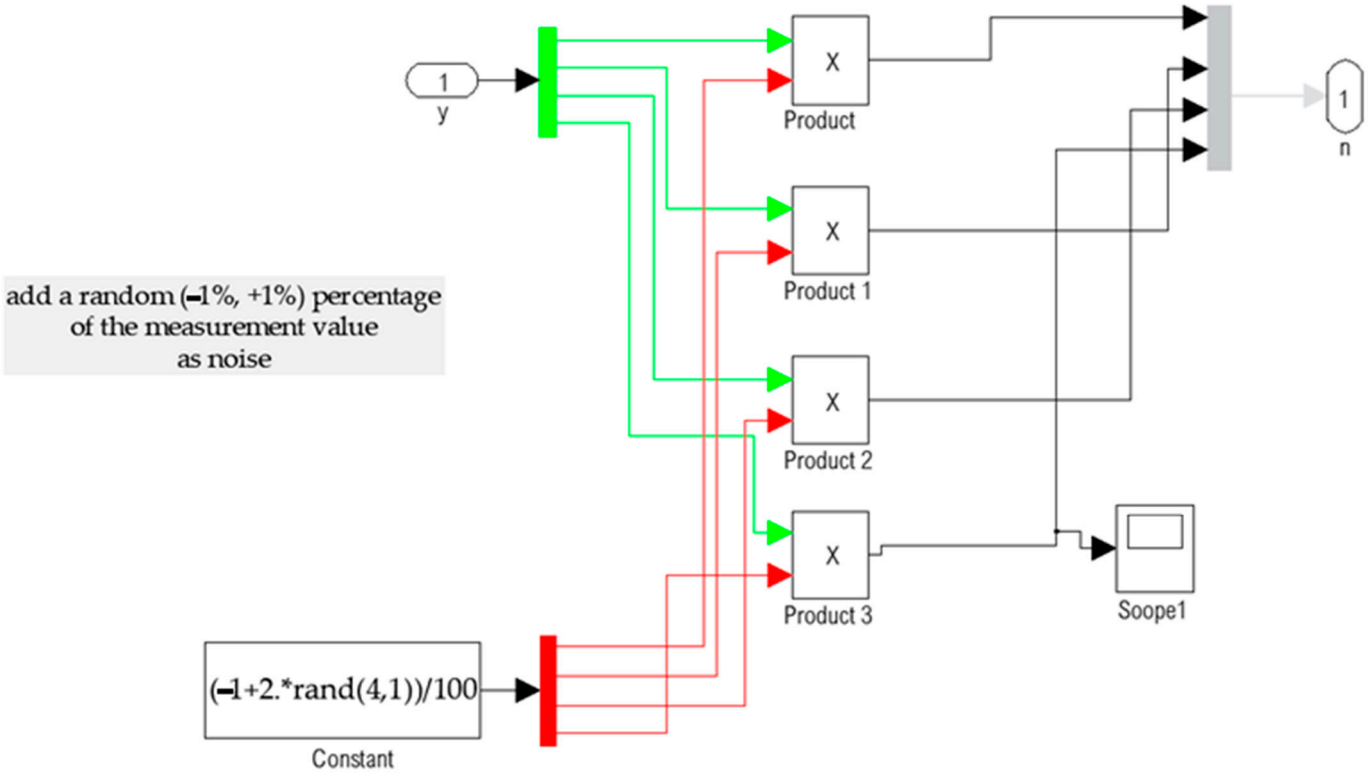

Figure 4. The block diagram in Simulink for the noise as a percentage of the measurement (* is × in the diagram).

All the simulations are in the Matlab program using the toolbox Simulink (Figure 5). The simulation has been done and the output of the result of the voltages (in volts) of the actuators can be seen. In all simulations, measurement noise has been taken as a percentage of the inputs as shown in Figures 4 and 5.

Figure 6 shows the beam's displacement over time as a result. In comparison to when there is no control, the displacement is almost zero. We were able to minimize vibrations by 95% by employing a unique control technique called H-infinity control. The green line is with H-infinity control (closed loop), and the red line is without control (open loop). Suppression of oscillations is achieved in all actuators and displacements are almost zero. This is very important in all mechanical constructions and a real innovation. At the same time, as shown in Figure 7, a relatively low voltage is achieved in the actuators since the suppression is done with approximately 50 Volts while the actuators withstand 500 Volts. As shown in Figure 7, the voltage generated by the control system to operate the control is within the 500 Volt safe limit for the material being utilized. The blue line shows the voltages of the last node, the green of the previous one, the red of the second, and the pale blue of the first node.

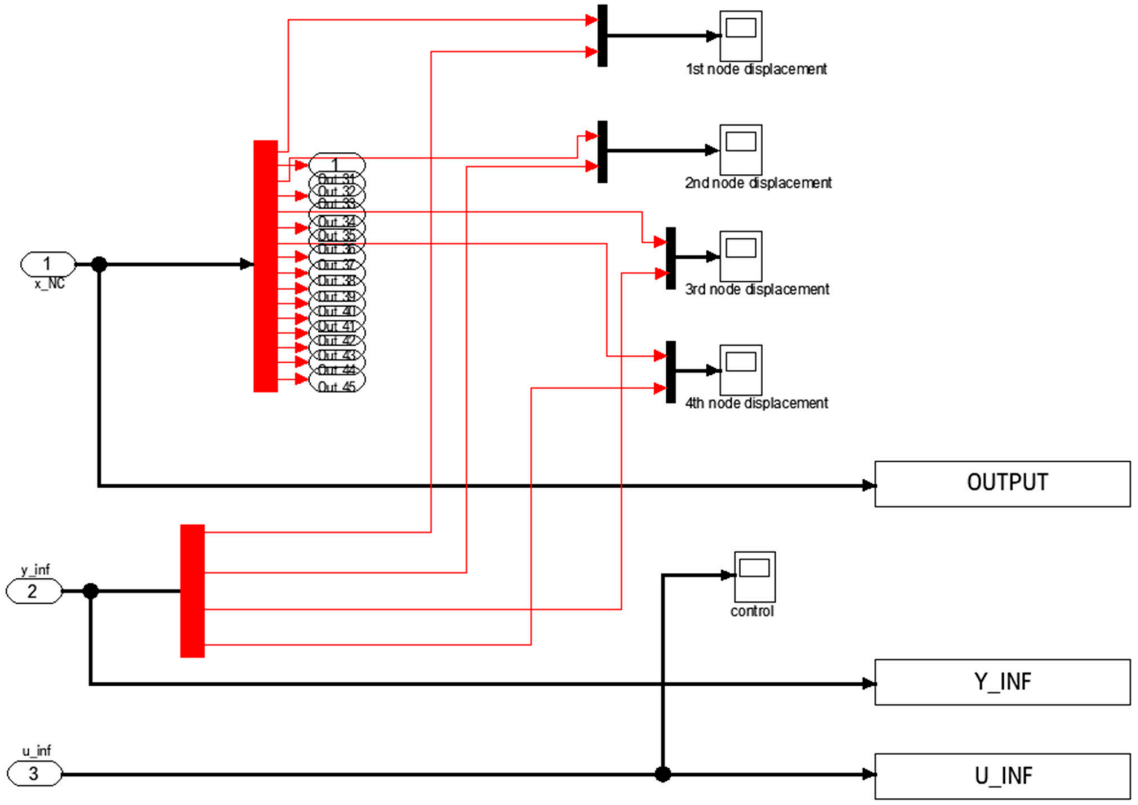

Figure 5. Simulation diagram for results in Matlab Simulink. The output is presented and explained in Figure 7 below.

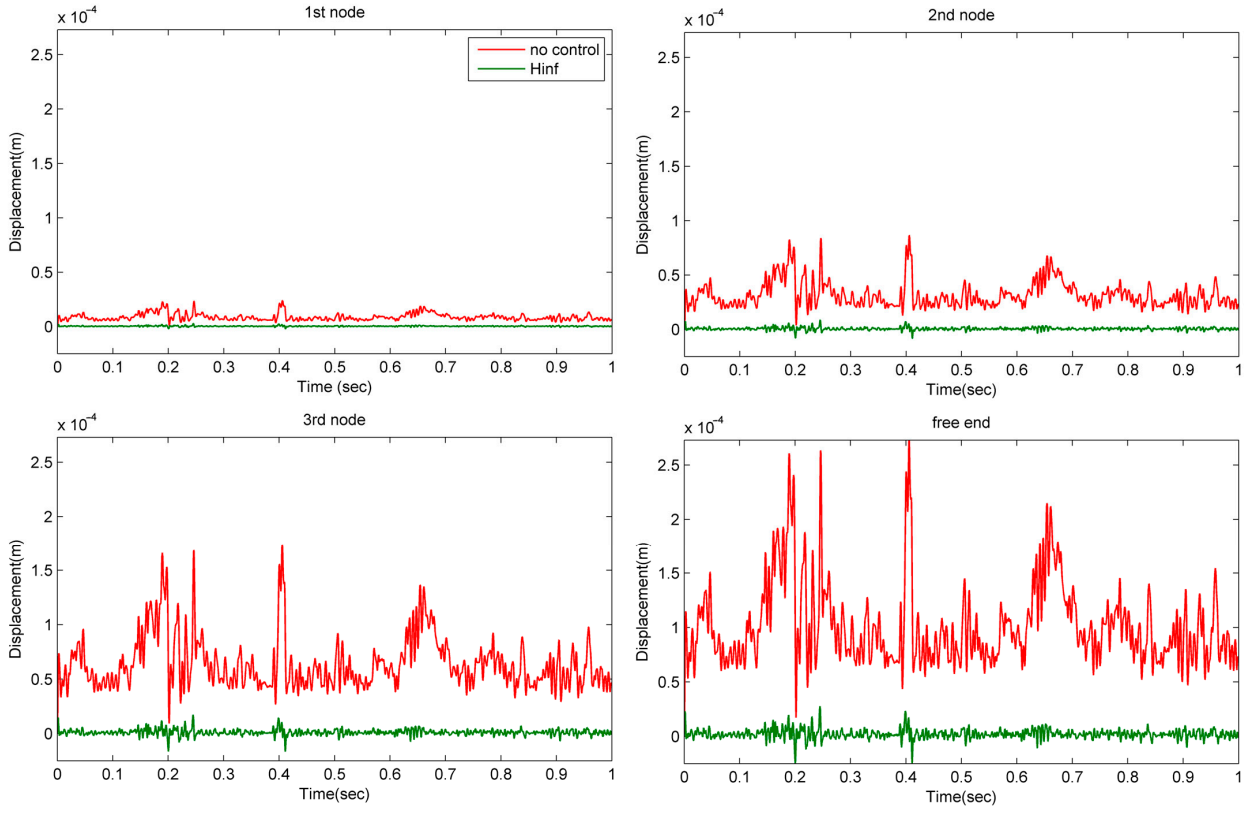

Figure 6. Displacements for the four nodes with actuators. The green line is with H-infinity control (closed loop), and the red line is without control (open loop).

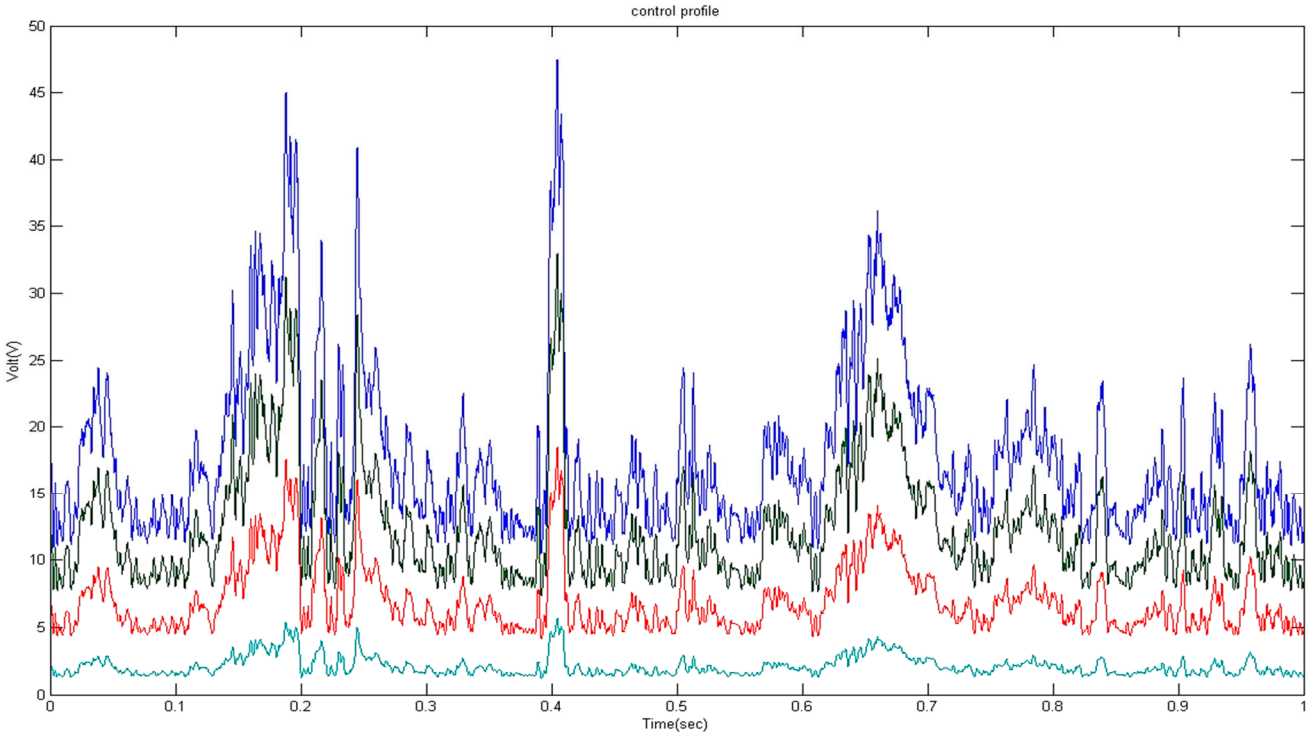

Figure 7. Control voltages for the four pairs of actuators of the beam. With the blue line is the control voltages for the free end of the smart beam, with green line the control voltages for the 3rd node of the smart beam, with red line the control voltages for the previous node of the smart beam and with the light blue line the first node of the smart beam.

In the frequency domain, Figure 8 shows graphs that represent the weight matrices. The results are obtained across the frequency range because oscillations must be classified at a specific value. The main advantage of H-infinite control is that we can work both in the time domain and the frequency domain. These matrices were made by doing a lot of tests to make sure we could find a controller. The controller that is made using H-infinity control has an order of 36. The value of γ for this controller is 0.074. The 36th order H-infinity controller was discovered. Because the order of the controller, which is equal to the order of the system, is typically higher than the order of conventional controllers like PI and LQR, researchers have developed order reduction techniques. The next method makes use of the Hifoo algorithm, which has been applied in the Matlab platform and is the most common of these algorithms.

The ultimate goal of the aforementioned system is to determine a controller of decreased rank/order n (36) while preserving the performance of the H-infinity criterion and a full-order controller's behavior [24,25,36,43,44]. The following are some advantages of this work: decline in order, complete suppression of oscillations, reduction of controller order, application of measurement noise of beam state, optimization of the H-infinity controller in intelligent structures, control of oscillation suppression through the simulation of intelligent entities, results in the time–space domain and the frequency domain, and input of white noise as disturbance input, taking it as a percentage of the disturbances. The outcomes are outstanding. With H-infinity control, we were able to obtain total rejections of disturbances.

3.3. Results for Hifoo Control

The Matlab routine for Hifoo control is:
Kfoo = hifoo (plant, 2)

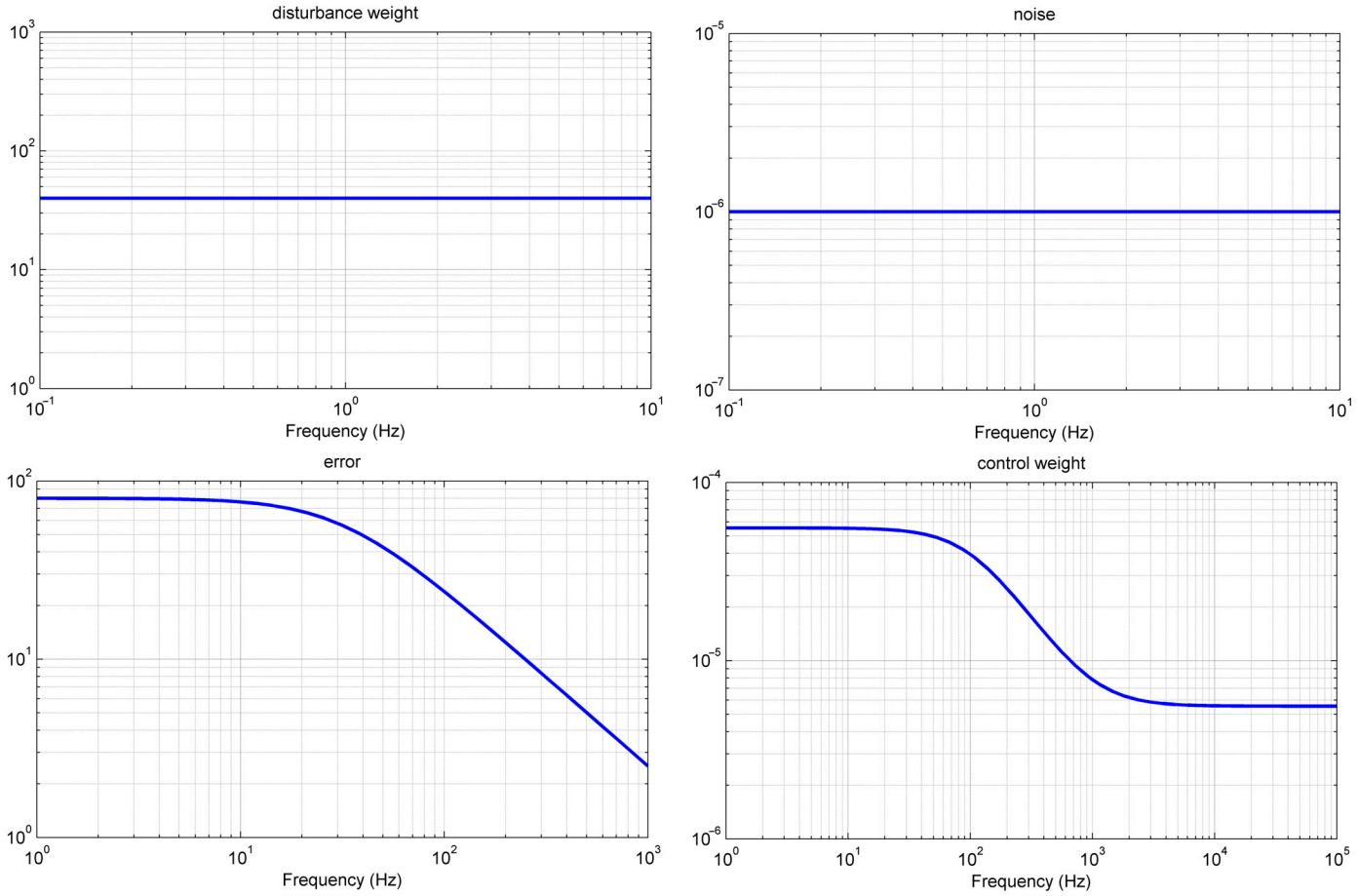

Figure 8. The Bode diagram in the frequency domain.

We employ a quasi-Newton technique (BFGS) to quickly estimate a local minimizer. Both the local bundle technique and the gradient sampling method are not employed if the MATLAB route does not include the quadratic programming tool "quadprog".

Where plants are the Equations (26) and (2) is the order of the controller, the matrices of the equation are:

$$\begin{aligned} \dot{x}_K(t) &= A_K\, x_K(t) + B_K y(t), \\ u(t) &= C_K\, x_K(t) + D_K y(t), \end{aligned} \tag{26}$$

$$\begin{aligned} A_{K=} &\begin{bmatrix} 828.1 & -5044 \\ 208.0 & -2408 \end{bmatrix} \\ B_{K=} &\begin{bmatrix} 412.8 & 911.6 & 1716 & 2810 \\ -164.9 & -637.2 & -1348 & -3207 \end{bmatrix} \\ C_{K=} &\begin{bmatrix} 1557 & -916.7 \\ 3013 & -592.3 \\ 627 & -297.9 \\ 144.3 & -92.59 \end{bmatrix} \\ D_{K=} &\begin{bmatrix} 76.1 & 6.6 & 287.1 & 468.3 \\ 23.5 & 87.69 & 186.5 & 303 \\ 12.12 & 44.12 & 93.39 & 154.3 \\ 4.204 & 12.53 & 26.92 & 783.51 \end{bmatrix} \end{aligned} \tag{27}$$

The control of beam position is achieved by displacing nodes on the order of 10^{-5} m, with the same output voltage, using the Hifoo controller for real wind loading. Therefore, even with a lower-order controller, we preserve H-infinity criteria performance. The Hifoo controller's maximum output voltage is 45 V, which is also true for the H_∞ controller. In other words, a lower-order controller that needs less voltage may adjust the beam to its

equilibrium point, as shown in Figure 9. The resultant displacement of the beam over time is seen in Figure 9 right. The displacement is nearly null as compared to when there is no control. By using a special control method known as H-infinity control, we were able to reduce vibrations by 95%. The red line is an open loop, whereas the green line has Hifoo control (closed loop). All actuators successfully suppress oscillations, and displacements are close to zero. In all mechanical structures, this is crucial and truly innovative. In addition, since the actuators can resist 500 Volts while the suppression is done with about 50 Volts, as illustrated in Figure 9 left, a reasonably low voltage is reached in the actuators. Figure 9 on the left displays the voltage produced. Even with the decreased order controller, the beam maintains balance. The blue line shows the voltages of the last node, the green of the previous one, the red of the second, and the pale blue of the first node. The control voltages fall below the 500 Volt piezoelectric limit [44–48].

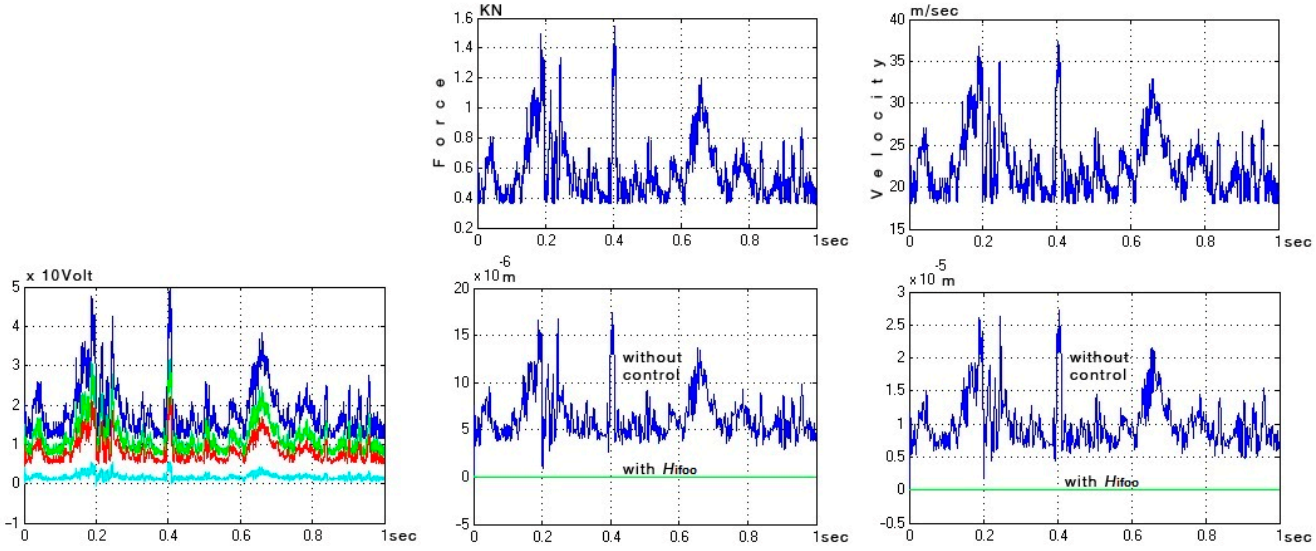

Figure 9. Control voltages and displacement response, of the middle and the free end of the beam with reduced-order control: Top two diagrams with the blue line is presented the wind force (top left diagram) and the wind velocity (top right diagram). Bottom three diagrams: For the bottom left diagram with the blue line is the control voltages for the free end of the smart beam, with green line the control voltages for the 3rd node of the smart beam, with red line the control voltages for the previous node of the smart beam and with the light blue line the first node of the smart beam. For the bottom right and middle diagram with blue line is the response without control and with green with Hifoo control.

The maximum singular values in the frequency domain, with and without the lowered order control are shown in Figure 10. The outcomes without control are shown by the blue line, and the green line is the results with control. For the above simulations, we apply a quasi-Newton technique (BFGS) for a quicker approximation of a local minimizer. Neither the local bundle technique nor the gradient sampling method is employed if the MATLAB route does not include the quadratic programming tool "quadprog". The gradients that Hifoo dynamically develops are utilized by each of these three optimization techniques. It is not attempted to locate the odd locations where gradients do not exist. The gradient discontinuities in unexpected locations do not cause the approaches to fail. A place where a convex combination of gradients at neighboring points has a small norm is sought in the last phases of the bundle and gradient sampling search parameter space. During the BFGS stage, an extremely ill-conditioned Hessian approximation matrix is generated. The local bundle technique or the gradient sampling method is not employed if the MATLAB route does not include the quadratic programming tool "quadprog". The gradients that Hifoo dynamically develops are utilized by each of these three optimization techniques. It is not attempted to locate the odd locations where gradients do not exist. The gradient

discontinuities in unexpected locations do not cause the approaches to fail. A place where a convex combination of gradients at neighboring points has a small norm is sought in the last phases of the bundle and gradient sampling search parameter space. During the BFGS stage, an extremely ill-conditioned Hessian approximation matrix is generated.

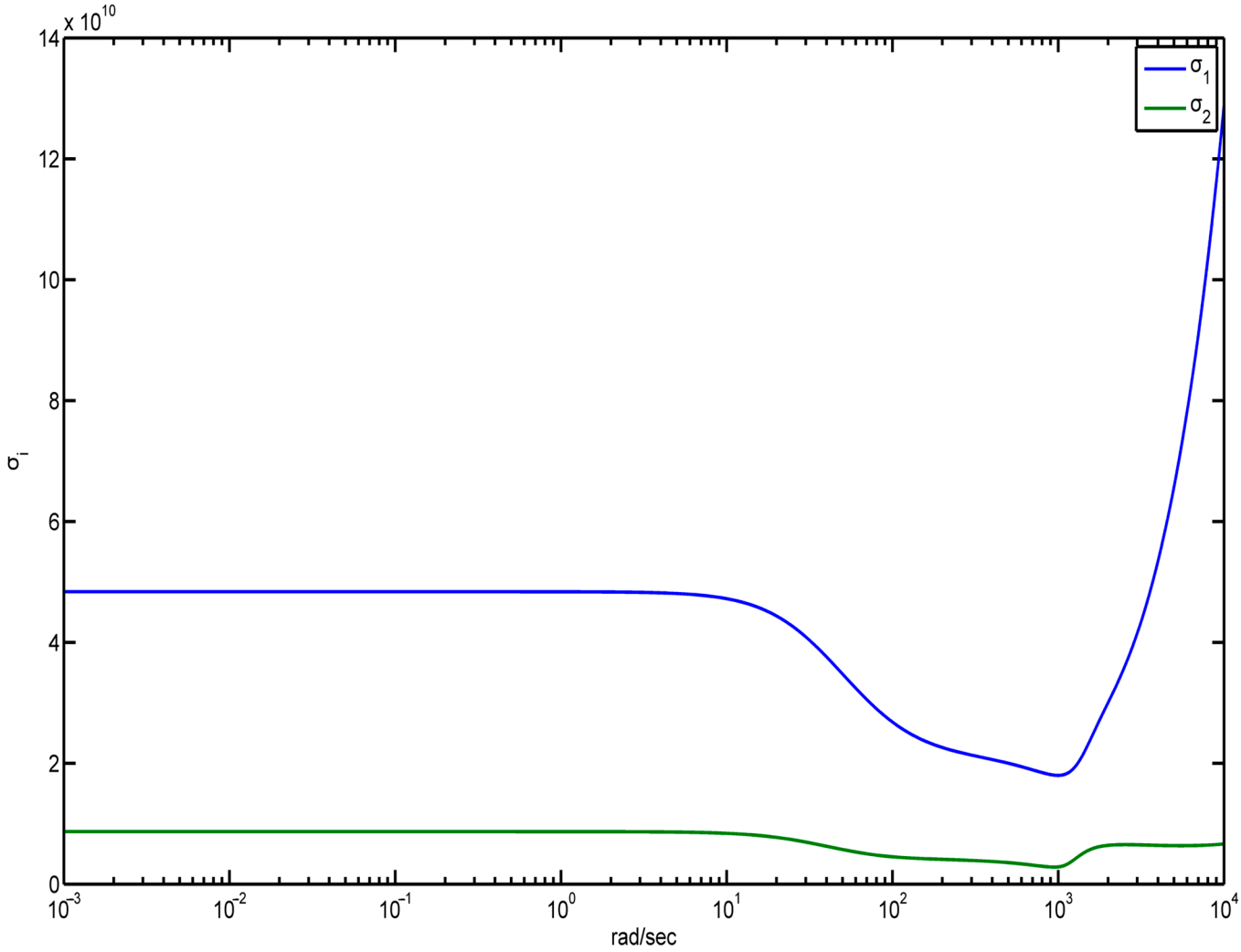

Figure 10. Structural singular values for reduced-order control.

4. Discussion

The current work has addressed the utilization of active control technologies in intelligent structures. Low steady-state error, quick recovery, and little-to-no maximum uplift are all desirable along with vibration reduction; nevertheless, control energy must not exceed operational limits [21,45,46]. The advantage of H-infinity control is that it enables the computation to take into consideration the worst-case scenario of disturbances with uncertainty and system noise [32,33,39,47]. Additionally, the H-infinity controller can efficiently handle greater input, allowing for the creation of a broad frequency spectrum. The results are significant; with piezoelectric component voltage controlled within tolerance, vibration reduction is shown even for genuine wind loads. By applying non-parametric and non-convex optimization techniques with the H_{IFOO} controller [5]. The model's processing requirements were reduced by lowering the controller rank. The controller worked properly even with a significantly lower system degree. Strong stabilization, which requires a controller that is self-stabilizing to stabilize a plant, and simultaneous stabilization, in which finding a single controller is required. To stabilize many plants, there are specific instances of multi-objective robust control issues [10,24,48]. Many important researchers

such as Crawley and de Louis [49] have dealt with smart materials and their inventions in construction. In this research, these materials are applied with advanced control techniques in the suppression of oscillations. Control and optimization on manufacturing processes and structures was also applied by various researchers afterward [50–53]. Most of the methods or heuristics that are currently used to address these issues usually lead to very high-order controllers as well. The outcomes demonstrate the utility of the suggested model and methodology, and the beam's control behavior conforms to expectations. The acknowledgment of new scientific issues that can serve as the foundation for study outside the purview of this work is a logical outcome of the suggested research advances. The maximum frequency of vibration for the system belongs to the high frequencies up to 10,000 Hz. Here, very good results are achieved in both high and low frequencies. The following are the outcomes of this work: a lowered order, the complete suppression of oscillations, reduction of controller order, optimization of the H-infinity controller in intelligent structures, and control of oscillation suppression by simulating intelligent entities, resulting in the time–space domain and the frequency domain, application of measurement noise of beam state, the input of white noise as disturbance input, taking it as a percentage of the disturbances, and application of measurement noise [25,36,44]. The outcomes are acceptable; using H-infinity control and reduced-order control, we completely reject disturbances. The different control methods used to lessen structural vibration and noise are referred to above. This investigation helps to apply controls to lessen the oscillations of intelligent structures. The major development is that complete oscillation suppression is accomplished with a reduced-order controller. In other words, the best outcome is obtained with significantly lower computing costs and without sacrificing any of the model's accuracy. In particular, experimental verification of the excellent results gained in the study of control might be a future research area.

5. Conclusions

Specific examples of multi-objective robust control problems are simultaneous stabilization, where a single controller must be created to stabilize a number of plants, and robust stabilization entails the requirement that a controller, in order to stabilize a plant, must also be inherently stable itself. In addition, the majority of the present methods or heuristics for resolving these problems frequently result in controllers of exceptionally high order. The beam's control behavior matches predictions, and the results show how useful the recommended model and methods are. Following a system analysis, we assess the system's usability and robustness.

The research investigates the positive aspects of robust control in intelligent systems by showing the use of H-infinity regulation and Hifoo optimization in both the state space and the frequency domain. These are the benefits of this work: order reduction optimization of the H-infinity controller in smart structures, control in oscillation suppression by modeling of intelligent entities, results in the time–space domain and the frequency domain, application of the measurement noise of the state of the beam, complete suppression of oscillations, reduction of the order of the controller, and the input of white noise as the disturbance input taking it as a percentage of the disturbances, to achieve the results programming has been done in Matlab. We employ a quasi-Newton technique (BFGS) to estimate a local minimizer more quickly. If the MATLAB route does not include the quadratic programming tool "quadprog", neither the local bundle technique nor the gradient sampling method is employed. These three optimization techniques each make use of the gradients that Hifoo dynamically produces. Finding the odd locations where gradients do not exist is not attempted. The positions of the gradient discontinuities do not cause the procedures to fail. The latter phases of the bundle and gradient sampling look for a place where a convex combination of gradients at neighboring points has a small norm. This technique helps to decrease the oscillations of intelligent structures by applying control. The breakthrough is the use of a reduced-order controller to completely suppress oscillations. In other words, the ideal outcome can be achieved with highly reduced processing needs and without

compromising the model's accuracy in any way. The focus of future studies will be on two areas; first, on how to apply these control mechanisms to real intelligent structures in an experimental scenario, and second, using alternative control strategies to suppress structural noise and vibration.

Author Contributions: G.E.S.: methodology; A.M. and M.P.: software, writing-review, and editing; N.V.: validation; M.P.: formal analysis; A.P.: investigation, software. All authors have read and agreed to the published version of the manuscript.

Funding: This research received no external funding.

Data Availability Statement: The data will be made available upon request to the corresponding author.

Acknowledgments: The authors are grateful for the support from Hellenic Mediterranean University and the Technical University of Crete.

Conflicts of Interest: The authors declare no conflict of interest.

References

1. Benjeddou, A.; Trindade, M.A.; Ohayon, R. New Shear Actuated Smart Structure Beam Finite Element. *AIAA J.* **1999**, *37*, 378–383. [CrossRef]
2. Bona, B.; Indri, M.; Tornambe, A. Flexible Piezoelectric Structures-Approximate Motion Equations and Control Algorithms. *IEEE Trans. Autom. Control* **1997**, *42*, 94–101. [CrossRef]
3. Okko, B.; Kwakernaak, H.; Gjerrit, M. *Design Methods for Control Systems*; Course Notes; Dutch Institute for Systems and Control: Delft, The Netherlands, 2001; Volume 67.
4. Burke, J.V.; Henrion, D.; Lewis, A.S.; Overton, M.L. HIFOO—A matlab package for fixed-order controller design and H∞ optimization. *IFAC Proc. Vol.* **2006**, *39*, 339–344. [CrossRef]
5. Burke, J.V.; Henrion, D.; Lewis, A.S.; Overton, M.L. Stabilization via Nonsmooth, Nonconvex Optimization. *IEEE Trans. Autom. Control* **2006**, *51*, 1760–1769. [CrossRef]
6. Burke, J.V.; Lewis, A.S.; Overton, M.L. A Robust Gradient Sampling Algorithm for Nonsmooth, Nonconvex Optimization. *SIAM J. Optim.* **2005**, *15*, 751–779. [CrossRef]
7. Burke, J.V.; Overton, M.L. Variational Analysis of Non-Lipschitz Spectral Functions. *Math. Program.* **2001**, *90*, 317–351. [CrossRef]
8. Choi, S.-B.; Cheong, C.-C.; Lee, C.-H. Position Tracking Control of a Smart Flexible Structure Featuring a Piezofilm Actuator. *J. Guid. Control Dyn.* **1996**, *19*, 1364–1369. [CrossRef]
9. Culshaw, B. Smart Structures—A Concept or a Reality? *Proc. Inst. Mech. Eng. Part I J. Syst. Control Eng.* **1992**, *206*, 1–8. [CrossRef]
10. Doyle, J.; Glover, K.; Khargonekar, P.; Francis, B. State-Space Solutions to Standard H2 and H∞ Control Problems. In Proceedings of the 1988 American Control Conference, Atlanta, GA, USA, 15–17 June 1988; pp. 1691–1696.
11. Tzou, H.S.; Gabbert, U. Structronics—A New Discipline and Its Challenging Issues. *Fortschr.-Ber. VDI Smart Mech. Syst.—Adapt. Reihe* **1997**, *11*, 245–250.
12. Tzou, H.S.; Anderson, G.L. *Intelligent Structural Systems*; Springer: Dordrecht, The Netherlands; Boston, MA, USA; London, UK, 1992; ISBN 978-94-017-1903-2.
13. Guran, A.; Tzou, H.-S.; Anderson, G.L.; Natori, M.; Gabbert, U.; Tani, J.; Breitbach, E. *Structronic Systems: Smart Structures, Devices and Systems*; World Scientific: Singapore, 1998; Volume 4, ISBN 978-981-02-2652-7.
14. Gabbert, U.; Tzou, H.S. IUTAM Symposium on Smart Structures and Structronic Systems. In Proceedings of the IUTAM Symposium, Magdeburg, Germany, 26–29 September 2000; Kluwer: Dordrecht, The Netherlands; Boston, MA, USA; London, UK, 2001.
15. Tzou, H.S.; Natori, M.C. *Piezoelectric Materials and Continua*; Braun, S., The Encyclopedia of Vibration, Eds.; Elsevier: Oxford, UK, 2001; pp. 1011–1018, ISBN 978-0-12-227085-7.
16. Cady, W.G. *Piezoelectricity: An Introduction to the Theory and Applications of Electromechanical Phenomena in Crystals*; Dover Publication: New York, NY, USA, 1964.
17. Tzou, H.S.; Bao, Y. A Theory on Anisotropic Piezothermoelastic Shell Laminates with Sensor/Actuator Applications. *J. Sound Vib.* **1995**, *184*, 453–473. [CrossRef]
18. David, C.; Sagris, D.; Petousis, M.; Nasikas, N.K.; Moutsopoulou, A.; Sfakiotakis, E.; Mountakis, N.; Charou, C.; Vidakis, N. Operational Performance and Energy Efficiency of MEX 3D Printing with Polyamide 6 (PA6): Multi-Objective Optimization of Seven Control Settings Supported by L27 Robust Design. *Appl. Sci.* **2023**, *13*, 8819. [CrossRef]
19. Moutsopoulou, A.; Stavroulakis, G.E.; Petousis, M.; Vidakis, N.; Pouliezos, A. Smart Structures Innovations Using Robust Control Methods. *Appl. Mech.* **2023**, *4*, 856–869. [CrossRef]
20. Cen, S.; Soh, A.-K.; Long, Y.-Q.; Yao, Z.-H. A New 4-Node Quadrilateral FE Model with Variable Electrical Degrees of Freedom for the Analysis of Piezoelectric Laminated Composite Plates. *Compos. Struct.* **2002**, *58*, 583–599. [CrossRef]

21. Packard, A.; Doyle, J.; Balas, G. Linear, Multivariable Robust Control With a μ Perspective. *J. Dyn. Syst. Meas. Control* **1993**, *115*, 426–438. [CrossRef]
22. Kim, S.-W.; Boo, C.-J.; Kim, S.; Kim, H.-C. Stable Controller Design of MIMO Systems in Real Grassmann Space. *Int. J. Control Autom. Syst.* **2012**, *10*, 213–226. [CrossRef]
23. Feng, Z.; Allen, R. Reduced Order H∞ Control of an Autonomous Underwater Vehicle. *IFAC Proc. Vol.* **2003**, *36*, 121–126. [CrossRef]
24. Chandrashekhara, K.; Varadarajan, S. Adaptive Shape Control of Composite Beams with Piezoelectric Actuators. *J. Intell. Mater. Syst. Struct.* **1997**, *8*, 112–124. [CrossRef]
25. Ackermann, J. *Robust Control, The Parameter Space Approach*; Springer: London, UK, 2002; ISBN 978-1-85233-514-4.
26. Gao, H.; Lam, J.; Wang, C. Controller Reduction with Error Performance: Continuous- and Discrete-Time Cases. *Int. J. Control* **2006**, *79*, 604–616. [CrossRef]
27. Yang, S.M.; Lee, Y.J. Optimization of Noncollocated Sensor/Actuator Location and Feedback Gain in Control Systems. *Smart Mater. Struct.* **1993**, *2*, 96. [CrossRef]
28. Ramesh Kumar, K.; Narayanan, S. Active Vibration Control of Beams with Optimal Placement of Piezoelectric Sensor/Actuator Pairs. *Smart Mater. Struct.* **2008**, *17*, 55008. [CrossRef]
29. Hanagud, S.; Obal, M.W.; Calise, A.J. Optimal Vibration Control by the Use of Piezoceramic Sensors and Actuators. *J. Guid. Control Dyn.* **1992**, *15*, 1199–1206. [CrossRef]
30. Song, G.; Sethi, V.; Li, H.-N. Vibration Control of Civil Structures Using Piezoceramic Smart Materials: A Review. *Eng. Struct.* **2006**, *28*, 1513–1524. [CrossRef]
31. Karatzas, I.; Lehoczky, J.P.; Shreve, S.E.; Xu, G.-L. Modeling, Control and Implementation of Smart Structures: A FEM-State Space Approach. Springer: London, UK, 1990; ISBN 9783540483939.
32. Miara, B.; Stavroulakis, G.E.; Valente, V. Topics on Mathematics for Smart Systems. In Proceedings of the European Conference, Rome, Italy, 26–28 October 2006; World Scientific Publishing: Singapore, 2006.
33. Moutsopoulou, A.; Stavroulakis, G.E.; Pouliezos, A.; Petousis, M.; Vidakis, N. Robust Control and Active Vibration Suppression in Dynamics of Smart Systems. *Inventions* **2023**, *8*, 47. [CrossRef]
34. Leibfritz, F. *COMPl e Ib: COnstrained Matrix-Optimization Problem Library—A Collection of Test Examples for Nonlinear Semidefinite Programs, Control System Design and Related Problems*; Universität Trier: Trier, Germany, 2001; pp. 1–23.
35. Wie, B.; Bernstein, D.S. Benchmark Problems for Robust Control Design. *J. Guid. Control Dyn.* **1992**, *15*, 1057–1059. [CrossRef]
36. Burke, J.V.; Lewis, A.S.; Overton, M.L. A Nonsmooth, Nonconvex Optimization Approach to Robust Stabilization by Static Output Feedback and Low-Order Controllers. *IFAC Proc. Vol.* **2003**, *36*, 175–181. [CrossRef]
37. Henrion, D.; Overton, M.L. Maximizing the Closed Loop Asymptotic Decay Rate for the Two-Mass-Spring Control Problem. *arXiv* **2006**, arXiv:math/0603681.
38. Henrion, D.; Sebek, M. Overcoming Non-Convexity in Polynomial Robust Control Design. In Proceedings of the Symposium on Mathematical Theory of Networks and Systems, Leuven, Belgium, 1 January 2004.
39. Zhang, N.; Kirpitchenko, I. Modelling Dynamics of A Continuous Structure with a Piezoelectric Sensoractuator for Passive Structural Control. *J. Sound Vib.* **2002**, *249*, 251–261. [CrossRef]
40. Vidakis, N.; Petousis, M.; Mountakis, N.; Moutsopoulou, A.; Karapidakis, E. Energy Consumption vs. Tensile Strength of Poly [Methyl Methacrylate] in Material Extrusion 3D Printing: The Impact of Six Control Settings. *Polymers* **2023**, *15*, 845. [CrossRef]
41. Vidakis, N.; Petousis, M.; Mountakis, N.; Papadakis, V.; Moutsopoulou, A. Mechanical Strength Predictability of Full Factorial, Taguchi, and Box Behnken Designs: Optimization of Thermal Settings and Cellulose Nanofibers Content in PA12 for MEX AM. *J. Mech. Behav. Biomed. Mater.* **2023**, *142*, 105846. [CrossRef]
42. Petousis, M.; Vidakis, N.; Mountakis, N.; Karapidakis, E.; Moutsopoulou, A. Functionality Versus Sustainability for PLA in MEX 3D Printing: The Impact of Generic Process Control Factors on Flexural Response and Energy Efficiency. *Polymers* **2023**, *15*, 1232. [CrossRef] [PubMed]
43. Kwakernaak, H. Robust Control and H∞-Optimization—Tutorial Paper. *Automatica* **1993**, *29*, 255–273. [CrossRef]
44. Blondel, V.D.; Tsitsiklis, J.N. A Survey of Computational Complexity Results in Systems and Control. *Automatica* **2000**, *36*, 1249–1274. [CrossRef]
45. Zhang, X.; Shao, C.; Li, S.; Xu, D.; Erdman, A.G. Robust H∞ Vibration Control for Flexible Linkage Mechanism Systems With Piezoelectric Sensors And Actuators. *J. Sound Vib.* **2001**, *243*, 145–155. [CrossRef]
46. Stavroulakis, G.E.; Foutsitzi, G.; Hadjigeorgiou, E.; Marinova, D.; Baniotopoulos, C.C. Design and Robust Optimal Control of Smart Beams with Application on Vibrations Suppression. *Adv. Eng. Softw.* **2005**, *36*, 806–813. [CrossRef]
47. Kimura, H. Robust Stabilizability for a Class of Transfer Functions. *IEEE Trans. Autom. Control* **1984**, *29*, 788–793. [CrossRef]
48. Francis, B.A. *A Course in H∞ Control Theory*; Springer: Berlin/Heidelberg, Germany, 1987; ISBN 978-3-540-17069-3.
49. Crawley, E.F.; de Luis, J. Use of piezoelectric actuators as elements of intelligent structures. *AIAA J.* **1987**, *25*, 1373–1385. [CrossRef]
50. Stavropoulos, P.; Chantzis, D.; Doukas, C.; Papacharalampopoulos, A.; Chryssolouris, G. Monitoring and Control of Manufacturing Processes: A Review. *Procedia CIRP* **2013**, *8*, 421–425. [CrossRef]
51. Turchenko, V.A.; Trukhanov, S.V.; Kostishin, V.G.; Damay, F.; Porcher, F.; Klygach, D.S.; Vakhitov, M.G.; Lyakhov, D.; Michels, D.; Bozzo, B.; et al. Features of Structure, Magnetic State and Electrodynamic Performance of $SrFe_{12-x}In_xO_{19}$. *Sci. Rep.* **2021**, *11*, 18342. [CrossRef]

52. Almessiere, M.A.; Slimani, Y.; Algarou, N.A.; Vakhitov, M.G.; Klygach, D.S.; Baykal, A.; Zubar, T.I.; Trukhanov, S.V.; Trukhanov, A.V.; Attia, H.; et al. Tuning the Structure, Magnetic, and High Frequency Properties of Sc-Doped $Sr_{0.5}Ba_{0.5}Sc_xFe_{12-X}O_{19}/NiFe_2O_4$ Hard/Soft Nanocomposites. *Adv. Electron. Mater.* **2022**, *8*, 2101124. [CrossRef]
53. Zaszczyńska, A.; Gradys, A.; Sajkiewicz, P. Progress in the applications of smart piezoelectric materials for medical devices. *Polymers* **2020**, *12*, 2754. [CrossRef]